Annals of Biomedical Engineering, Vol. 35, No. 11, November 2007 (© 2007) pp. 2003–2022
DOI: 10.1007/s10439-007-9361-3

A Mathematical Model of Human Respiration at Altitude

MATTHEW BERNARD WOLF[1] and ROBERT P. GARNER[1,2]

[1]Department of Pharmacology, Physiology and Neuroscience, University of South Carolina School of Medicine, 6439 Garners Ferry Road, Columbia, SC 29209, USA; and [2]Odyssey II Solutions, Wichita, KS 67208, USA

(*Received 17 November 2006; accepted 18 July 2007; published online 3 August 2007*)

Abstract—We developed a mathematical model of human respiration in the awake state that can be used to predict changes in ventilation, blood gases, and other critical variables during conditions of hypocapnia, hypercapnia and these conditions combined with hypoxia. Hence, the model is capable of describing ventilation changes due to the hypocapnic-hypoxia of high altitude. The basic model is that of Grodins et al. [Grodins, F. S., J. Buell, and A. J. Bart. *J. Appl. Physiol.* 22:260–276, 1967]. We updated the descriptions of (1) the effects of blood gases on cardiac output and cerebral blood flow, (2) acid–base balance in blood and tissues, (3) O_2 and CO_2 binding to hemoglobin and most importantly, (4) the respiratory-chemostat controller. The controller consists of central and peripheral sections. The central chemoceptor-induced ventilation response is simply a linear function of brain P_{CO_2} above a threshold value. The peripheral response has both a linear term similar to that for the central chemoceptors, but dependent upon carotid body P_{CO_2} and with a different threshold and a complex, nonlinear term that includes multiplication of separate terms involving carotid body P_{O_2} and P_{CO_2}. Together, these terms produce 'dogleg'-shaped curves of ventilation plotted against P_{CO_2} which form a fan-like family for different values of P_{CO_2}. With this chemical controller, our model closely describes a wide range of experimental data under conditions of solely changes in P_{CO_2} and for short-term hypoxia coupled with P_{CO_2} changes. This model can be used to accurately describe changes in ventilation and respiratory gases during ascent and during short-term residence at altitude. Hence, it has great applicability to studying O_2-delivery systems in aircraft.

Keywords—Mathematical model, Human respiration, Hypercapnia, Hypocapnia, Hypoxia, Altitude hypoxia.

ABBREVIATIONS, SYMBOLS AND TERMINOLOGY

HCO_3	Bicarbonate
C	Content or concentration, L gas 100 L blood^{-1}
CSF	Cerebrospinal fluid
H	Hematocrit, fractional
HbCO	Carbamino hemoglobin
mM	Concentration, millimoles L^{-1}
MR	Metabolic rate, mL min^{-1}
P	Gas partial pressure, torr
Q	Blood flow, L min^{-1}
RQ	Respiratory Quotient
S	Hemoglobin O_2 saturation, fractional
SF	Shunt fraction
T	Respiratory threshold, torr
V	Volume, L
$\dot{V}$	Ventilation, L min^{-1}
f	Fraction
α	Gas solubility, mM L blood^{-1}
t	time, s

Subscripts and superscripts

A	Alveolar
a	Arterial
b	Brain
bl	Blood
cb	Carotid body
D	Deadspace
et	End tidal
I	Inspiratory (ventilation)
pl	Plasma
rc	Red blood cell
ti	Tissue
T	Tidal (volume)
v	Venous

INTRODUCTION

The introduction of transport aircraft that could routinely attain high altitudes in the 1950s produced the possibility that humans might be exposed to dangerous environmental conditions if there was a failure of the cabin pressurization system. Even now,

Address correspondence to Matthew Bernard Wolf, Department of Pharmacology, Physiology and Neuroscience, University of South Carolina School of Medicine, 6439 Garners Ferry Road, Columbia, SC 29209, USA. Electronic mail: wolf@med.sc.edu

decompression of passengers to operational limits may happen on commercial aircraft. The resulting low temperatures and low O_2 pressures can only be tolerated briefly.

The primary protection against altitude-induced hypoxia is the cabin pressurization system. In case of failure of this system, commercial passenger airliners are equipped with onboard systems that deliver oxygen through masks. These masks are designed for rapid donning in an emergency to attenuate the effects of hypoxia. These systems are designed to cope with this situation, but evaluation and optimization of new concepts and designs is relatively limited due to the number of possible variations and the number of human altitude exposures that may be required. An alternative is to use mathematical models of the human respiratory system to evaluate these systems in a manner that provides additional support to machine and human-subject test requirements. However, these models must be sufficiently complex to describe transient human respiratory responses at altitude and they must be fully validated to provide confidence in their predictions.

Complex respiratory-chemostat models were devised in the 1950s and 1960s by Grodins and others.[19] Early model complexity, limited by the inadequacy of analog computers, was circumvented by the strides in digital computing in the 1960s. Grodins's digital computer model of 1967[18] stands to this day as a basis for any model of the respiratory-chemostat plant, because it includes the recognized important chemical and physical processes necessary to describe human respiratory behavior. Mainly lacking in Grodins's model was an accurate description of the respiratory controller, which transduces chemical signals into ventilation. In fact, such a description was the ultimate object of Grodins's work.

Grodins used his model[18] with some hypothesized controller formulations to examine its qualitative responses to hypercapnia, hypoxia, and altitude and concluded that it had the capability of adequately describing these conditions. However, he did not seek quantitative comparison with experimental data, which is proof of the validity of any model. Such evidence was sought in his previous model[19] of CO_2 control. Over the intervening 40 years, there have been a number of models of respiratory control. Notable advances have been made in the last few years.[30,46–48] However, the fundamental characteristics of the Grodins model are still recognized as being the foundation upon which refinements must be built.

Unfortunately, out of the numerous models of respiratory behavior, we have found none that can adequately describe the respiratory response to the high altitude-induced stress of hypocapnic-hypoxia because of either inadequate validation or the use of respiratory controller equations that do not yield realistic ventilatory predictions during severe hypocapnia. Hence, we devised a new model, based on Grodins' respiratory plant model, but updated with improvements from recent models and with a respiratory controller function that could handle the high altitude-induced hypocapnic-hypoxia condition under awake conditions.

Even though hypercapnia usually is not an issue at altitude, we decided to initially validate the model predictions under this condition because of the large amount of human experimental data available and because it tested the validity of most of the model structure. Then, the model predictions were tested under hypoxic conditions with many variations, such as coupled with hypercapnia, hypocapnia, etc. depending upon available human data. Finally, we looked at the limited amount of data for unacclimatized man during transient altitude exposure and then used the model to make some predictions under various scenarios. Our aim is the simulation of short-term (< 10 min) altitude exposure to hypoxia in aircraft because oxygen masks are normally donned well within this time to prevent the effects of hypoxia. Hence, the data from numerous studies where hypoxia was imposed for much longer times are not considered, including the effects of acclimatization. Consequently, the phenomenon of hypoxic ventilatory depression (HVD)[27,45] was not specifically simulated in the present model, even though this centrally-mediated response may begin within the 10-min time frame of interest.

In this initial study, only effects of hydrogen-ion concentration on O_2 and CO_2 binding to hemoglobin are included because effects of acid–base changes on respiratory control are not important in the short-term control focus of this study. However, we did include a preliminary description of tissue acid–base behavior for use in future applications of the model.

METHODS

The most important new contribution of this study is the formulation of a respiratory controller that can accurately predict the changes in ventilation due to variations in CO_2 and O_2 gas tensions at sea level and at high altitudes. Hence, it is informative to present a short review of historical development of such formulations and to point out some shortcomings that guided our present approach.

The first quantitative approach to describing chemical control of breathing was by Gray[17] in 1946. His multiple factor hypothesis described ventilation as the sum of individual effects of arterial O_2, CO_2, and H^+. However, his approach did not explain data on

the interaction of O_2 and CO_2 on ventilation as noted by Lloyd and Cunningham[28] in 1963. They specifically pointed to two sets of data not well explained by Gray's hypothesis, (1) the hyperbolic relationship between steady-state ventilation and P_{O_2} at constant, but elevated, P_{CO_2}, as measured by Cormack *et al.*[4] and (2) the 'dog leg'- or 'hockey stick'-shaped curves of steady-state ventilation vs. P_{CO_2} at constant P_{O_2} measured by Nielsen and Smith.[31] However, it should be noted that the data of Cormack *et al.* was highly variable and Lloyd and Cunningham only chose the data of one subject to display. Similarly, the data of Nielsen and Smith shown was for only one of their two subjects. Nevertheless, this latter data set has been cited since then in many publications, including the chapter by Cunningham *et al.*[7] in the Handbook of Respiration, as quantitative representation of human respiratory responses to changes in alveolar (blood) gas tensions.

Lloyd and Cunningham[28] proposed a nonlinear equation with four parameters that qualitatively described the behavior of those data sets at P_{CO_2} values above 'resting.' 'Resting' is presumably defined as the P_{CO_2} value at the knee of the dog leg. The resulting family of curves was a series of fan-shaped lines of steady-state ventilation (so called 'Oxford' fan) vs. P_{CO_2} whose slopes increased with decreasing values of P_{O_2} and meeting at a single point. The low P_{CO_2} part (nearly flat ventilation changes) of the Nielsen and Smith[31] data was not addressed. Lloyd and Cunningham tried to identify the values of these parameters under a range of conditions with a limited degree of success. In 1974, Severinghaus[41] proposed a rapid experimental protocol for measuring these four parameters and a fifth parameter, the point of intersection of the lines. However, there is yet no agreement on normal parameter values, suggesting that a simple equation with arterial (alveolar) concentrations as the independent variables may not be sufficient to describe steady-state ventilation.

Cunningham[6] in 1974 proposed that the shape of the ventilation vs. P_{CO_2} data of Nielsen and Smith[31] might be explained by a CO_2, H^+ central stimulation of ventilation added to a CO_2, H^+ peripheral stimulation modulated by hypoxia. Such a description was incorporated by Duffin[10] in 1972 in his model of the chemical control of ventilation. Indeed, his model yielded steady-state controller curves with distinct similarities to those of Cormack *et al.*[4] and Nielsen and Smith.[31] However, computer limitations restricted the required complexity of his lung model. Subsequent numerous models[25,30,46–48] have generally adopted the idea that the ventilatory controller has inputs from both central and peripheral receptors that are additive and that the nonlinear interaction between CO_2 and O_2 occurs peripherally.

In the present study, the aviation focus required prediction of transient ventilatory responses for ascent to high altitudes. Hence, the model had to predict ventilation changes to the combined stress of hypoxia and the resulting hypocapnia induced by the hyperventilation. It was clear to us that the steady-state controller equation proposed by Severinghaus[41] was inadequate because it predicted ventilations of zero and below at P_{CO_2} values less than about 35–37 torr. In contrast, we expected to study scenarios in which this value fell below 20 torr. The formulation by Duffin[10] was capable of realistic predictions at such low values in contrast to formulations in most other models. Hence, we adopted his strategy, but with some significant modifications. (1) For simplicity, Duffin used arterial concentrations for his variables, whereas we used concentrations specific to receptor sites, i.e., carotid body and brain, (2) Duffin assumed that both the peripheral and central chemoceptor output signals were rectangular-hyperbolic functions of O_2 and CO_2, whereas we used linear functions of CO_2 and a hyperbolic function of O_2 (see Eqs. 9 and 10), and (3) Duffin did not validate his formulation by comparing his model predictions to experimental data, whereas our intent is to present extensive evidence of the validity of our formulation.

Model Formulation

The basic model of the respiratory chemostat plant is that of Grodins *et al.*[18] and will not be repeated in detail for this paper. Briefly, O_2 and CO_2 concentrations are computed from differential equations derived from mass balance in three compartments, lung, brain, and remaining tissues. Arterial and venous blood gases are assumed to be in equilibrium with those determined in these compartments. Variable transportation delays are computed using the approach and segment volumes given by Grodins *et al.*[18]

However, there are a number of areas where new data or better approaches are available, allowing us to update the plant and controller formulations. These are explained below.

O_2-Hemoglobin Saturation Curves

There are a number of invertible analytic expressions which can accurately describe this curve in arterial and venous blood, but they fail at both very high and low P_{O_2}. Since the new model has to deal with both low O_2 tensions and breathing 100% O_2, we used a piecewise linear fit to tabulated data[42] over the range of 0–760 torr. Shifts of the curves with temperature, pH, and P_{CO_2} were obtained as by Lobdell.[29] Hence, computations of arterial and venous blood pH are required in the model.

CO_2-Hemoglobin Dissociation Curve

We derived an empirical fit to the data of Comroe[3]

$$C_{CO_2} = 12.6*(P_{CO_2})^{0.396}\times(1-0.117*S) \quad (1)$$

where C_{CO_2} is total CO_2 concentration in arterial (a) or venous (v) blood in L CO_2 100 L^{-1} blood and S refers to fractional O_2 hemoglobin saturation in that fluid.

Acid–Base Changes

Blood

Arterial-plasma pH (pH_{pl}) values and tissue and brain venous-plasma pH values were determined using the Henderson–Hasselbach equation. In this equation, plasma bicarbonate (HCO_3) concentration was obtained by subtracting from total blood CO_2 (Eq. 1) the CO_2 contribution by red cells using the approach of Davenport.[8] The resulting equation is

$$pH_{pl} = 6.1 + LOG_{10}\left(\frac{C^{bl}_{CO_2} - C^{rc}_{HCO_3} - C^{rc}_{HbCO} - [H\times\alpha^{rc}_{CO_2} + (1-H)\times\alpha^{pl}_{CO_2}]\times P^{pl}_{CO_2}}{(1-H)\times\alpha^{pl}_{CO_2}\times P^{pl}_{CO_2}}\right) \quad (2)$$

where plasma and red cell CO_2 solubilites (αCO_2) are 0.0301 and 0.025 mM $torr^{-1}$, respectively, and fractional hematocrit (H) is 0.4. The contribution of red cell carbamino hemoglobin (HbCO) was also determined from data in Davenport as

$$C^{rc}_{HbCO} = 0.02 + 0.002\times P^{pl}_{CO_2} + 0.228\times(1-S) \quad (3)$$

Tissues

Brain and tissue (ti) P_{CO_2} values were determined from CO_2 dissociation data of dog brain.[24] We fit the data with the function

$$P_{bCO_2} = 33.92\times e^{0.0309\times C_{bCO_2}} - 44.88 \quad (4)$$

where C_{bCO_2} is in mL CO_2 (100 g brain)$^{-1}$. Although we did not need brain and tissue pH values for the present application, they were computed from the Henderson–Hasselbach equation[8] as

$$pH_b = 6.1 + \log_{10}\left(\frac{C_{bCO_2} - \alpha_{bCO_2}}{\alpha_{bCO_2}\times P_{bCO_2}}\right) \quad (5)$$

where α_{bCO_2} is 0.0309 mM $torr^{-1}$.

Blood Flow

Blood flow was described as a resting value multiplied by analytical functions of changes in arterial O_2 and CO_2.

Effects of O_2 and CO_2 on Cardiac Output

We fit analytical functions to cardiac output data from humans subjected to hypoxia and CO_2 changes by Richardson *et al.*[38–40] and Cullen and Eger.[5] The experimental data and the fit to the hypoxia-induced data are shown in the Appendix (Fig. A1). The composite equation derived is

$$Q = Q^0\times\left(0.937 + \frac{0.817}{1+\left(\frac{P_{aO_2}}{47.2}\right)^{3.41}}\right)\times Q(CO_2) \quad (6)$$

where Q^0 is the steady-state value in L min^{-1}. The set of terms in the brackets were scaled from the fit such that $Q = Q^0$ at rest. Q is always $\geq Q^0$. $Q(CO_2) = 1 + 0.03\times(P_{aCO_2} - 40)$ during hypercapnia and the 0.03 multiplying constant becomes –0.025 during hypocapnia. The response during hypocapnia is altered by a first-order, 250-s time constant.[38]

Effects of O_2 and CO_2 on Brain Blood Flow

We fit analytical functions as above to data on humans subjected to hypoxia from Shapiro *et al.*,[43] Kolb *et al.*,[26] and Cohen *et al.*[2] and we used the Reivich[35] fitting equation derived from data in rhesus monkeys subjected to hypo- and hypercapnia. The resulting equation is

$$Q_b = Q^0_b\times\left(1.014 + \frac{0.734}{1+\left(\frac{P_{aO_2}}{41.4}\right)^{16.6}}\right)\times\left(0.43 + \frac{1.91}{1+10,600\times e^{-5.25\times\log_{10}P_{aCO_2}}}\right) \quad (7)$$

where Q^0_b is the steady-state brain blood flow. The set of terms in the brackets were scaled from the fit such that $Q_b = Q^0_b$ at rest. Q_b is always $\geq Q^0_b$. The experimental data and the fit during hypoxia are shown in the Appendix (Fig. A1). Dynamic changes in Q and Q_b flows were further slowed by first order, 15 and 6-s time constants,[18,46] respectively (see Discussion).

Lung Blood Flow

A fraction (SF) of the venous blood is shunted past the lungs whereas the remaining fraction (1–SF) passes through the lungs and is oxygenated. The O_2 content of the resulting arterialized blood is

$$C_{aO_2} = (1 - SF) \times C_{AO_2} + SF \times C_{vO_2} \quad (8)$$

where C_{AO_2} is the O_2 content of blood passing through the lung in equilibrium with alveolar (A) gas.

Ventilatory Control

The Grodins model[18] used alveolar ventilation explicitly in its formulation. In the present model, this ventilation is derived from inspiratory ventilation less the ventilation of the dead space derived from Eq. (13) (see below). The controller consists of central and peripheral components whose effects on total ventilation (often called minute ventilation) are *additive*. Both components are affected by CO_2, but only the peripheral one is affected by O_2. In contrast to Grodins and some others who added a constant resting-ventilation value to the chemostat-induced ventilation function, we decided to let the sensitivities and thresholds of the central and peripheral chemostats (four parameters) determine the resting ventilation (see Model Validation and Discussion).

Central Controller

The central (c) part of the controller senses brain P_{CO_2} (P_{bCO_2}). Centrally induced ventilation ($\dot{V}_c$) is assumed to be always positive and increases linearly with P_{bCO_2} above a threshold level (T_{bCO_2}). Its equation is

$$\dot{V}_c = K_{bCO_2} * (P_{bCO_2} - T_{bCO_2}), \quad \dot{V}_c \geq 0 \quad (9)$$

Peripheral Controller

The peripheral controller senses arterial blood–gas concentrations at the carotid body (P_{cbO_2} and P_{cbCO_2}). The positive peripheral (p) contribution to ventilation ($\dot{V}_p$) is formulated as

$$\dot{V}_p = K_{cbCO_2} \times (P_{cbCO_2} - T_{cbCO_2}) + \left[\frac{570}{P_{cbO_2} - 26.2} - 8.05\right] \times F(CO_2), \quad \dot{V}_p \geq 0 \quad (10)$$

The first set of terms in Eq. (10), similar to Eq. (9), is the *positive* peripheral contribution to the linear CO_2 response curve. The next set of terms is the *positive* hyperbolic increase in ventilation due to hypoxia. The function (F) of CO_2 is the inhibition or augmentation of the peripheral hypoxic drive due to changes in CO_2.

The form of the hyperbolic term in square brackets in Eq. (10), including the 26.2 torr constant shown, was taken from Severinghaus.[41] The 570 constant was determined to match the model's steady-state, hypoxic ventilatory response to that of extensive data by Reynolds et al. (see Model Validation). The 8.05 value was determined to yield a zero-ventilation effect at normal carotid-body O_2 tension.

The functions of CO_2 used in Eq. (10) are

$$F(CO_2) = \left[5 - 4 \times \left(\frac{P_{cbCO_2}}{P^0_{cbCO_2}}\right)^4\right]^{-1} \text{ for } \left(\frac{P_{cbCO_2}}{P^0_{cbCO_2}}\right) \leq 1$$
$$F(CO_2) = \left(\frac{P_{cbCO_2}}{P^0_{cbCO_2}}\right)^3 \text{ for } \left(\frac{P_{cbCO_2}}{P^0_{cbCO_2}}\right) > 1 \quad (11)$$

where $P^0_{cbCO_2}$ is the resting value. This set of functions produces a family of curves of total ventilation as a function of both O_2 and CO_2 commonly characterized as dog-leg shaped and fan like.[20] The rationale for the functions chosen is described in Model Validation and Discussion.

The ventilatory response induced by the peripheral chemoceptors was slowed by a 35-s time constant. This value was determined to match the ventilatory response (Fig. 6) to a brief hypoxia followed by hyperoxia.[15] The mechanism of these dynamics is called short-term potentiation or neural afterdischarge (see Discussion).

Determination of Tidal Volume

Tidal volume (V_T) was derived from inspiratory (I) ventilation ($\dot{V}_I$) using data from the literature fit by the following equation

$$V_T = 0.152 \times (\dot{V}_I)^{0.683} \quad (12)$$

where V_T is in L and $\dot{V}_I$ is in L min^{-1}. The experimental data and the fit are shown in the Appendix (Fig. A2). Since the experimental data were only for V_T greater than about 0.5 L, this approximation may be increasingly inaccurate at lower values.

Dead Space (Implicitly Constant in Grodins et al.[18] original formulation)

Dead-space volume (V_D) is described using a cylindrical airspace model with laminar flow wash out[20] as

$$V_D = (0.18 + 0.023 \times V_T) \times \left(1 - \frac{0.18 + 0.023 \times V_T}{4 \times V_T}\right) \quad (13)$$

Validation Experimental Protocol

The model was validated over a wide range of conditions against human data in the awake state, including hypercapnia or hypoxia alone or hypoxia coupled with either hypocapnia or hypercapnia to

show that its ability of accurate prediction was not limited to a narrow focus as in many previous studies. Although our primary intent was to predict experimental changes in ventilation, comparison was also made to blood-gas tensions and other respiratory variables when these data were available.

For the normal (resting) steady state and hypercapnic conditions, there were four parameters whose values had to be selected, the gains and threshold values of the central and peripheral chemoceptors (Eqs. 9 and 10). These were selected to (1) yield a resting alveolar ventilation in the range suggested by Grodins, (2) yield a resting P_{ACO_2} of 40 torr, (3) match the maximum ventilation achieved after 25 min of 7% CO_2 inhalation in the study of Reynolds et al. below, and (4) have a CO_2 response gain of peripheral chemoceptors of ~50% of that of the central ones as suggested by Bellville *et al.*[1]

Resting Steady state

The steady-state values of the variables were determined by running the model for 60 min. The results were examined to see if the solution was stable and to compare the values with the simulation results of Grodins et al.[18] for a normal, resting, awake individual (Table 1).

Hypercapnic Steady state

We compared the simulation predictions with data of ventilation and P_{ACO_2} from numerous studies where the subjects inhaled hypercapnic gas mixtures for various lengths of time, usually less than 30 min. Since steady-state ventilation increases typically take > 30 min to be achieved,[19] comparisons were made with model-predicted transient data at the times the experimental data were measured (Fig. 1).

TABLE 1. Resting steady-state values.

		Normal control	
Variable	Units	Present study	Grodins *et al.*[18]
$\dot{V}_I$	L min^{-1}	7.36	
$\dot{V}_c$	L min^{-1}	6.04	
$\dot{V}_p$	L min^{-1}	1.32	
$\dot{V}_A$	L min^{-1}	5.15	5.05–5.35
V_D	L	0.593	
P_{AO_2}	torr	105	105.5–108
P_{aO_2}	torr	97.0	
P_{bO_2}	torr	33.8	36.5–37.3
P_{tO_2}	torr	42.1	46.7–47.2
S_aO_2	%	97.4	
P_{ACO_2}	torr	40.0	37.5–39.7
P_{bCO_2}	torr	51.3	47.8–50.2
P_{tCO_2}	torr	45.6	42.3–44.7
pH_a		7.40	7.41–7.43
pH_{vt}		7.36	7.38–7.4
Q	L min^{-1}	6.00	6.00
Q_b	L min^{-1}	0.75	0.75

CO_2-Inhalation (Hypercapnia)

Reynolds *et al.*[37] measured transient data for ventilation, gas tensions, tidal volume and respiratory rate for 25 min of 3, 5, 6, and 7%-CO_2 inhalation. Their ventilation and tidal volume experimental data were standardized to a body surface area of 1.73 m^2. This standardization reduced resting ventilation values to 5.7–6.3 L min^{-1} and tidal volume values to 0.58–0.61 L for the four sets of data. Hence, their transient ventilation data were rescaled to our higher resting value (7.36 L min^{-1}) given in Table 1. We compared our model predictions to all these data, except respiratory rate, since it can be derived directly from ventilation and tidal volume (Fig. 2).

End Tidal (et) CO_2 Step Increase

Bellville *et al.*[1] measured transient ventilation data with P_{etCO_2} clamped first at eucapnia, then during a step increase and finally back to eucapnia. This maneuver was in normal subjects and with subjects whose carotid bodies (CB) had been resected. The magnitude of the hypercapnic step was not given; only the end pressure was given. Hence, we computed the

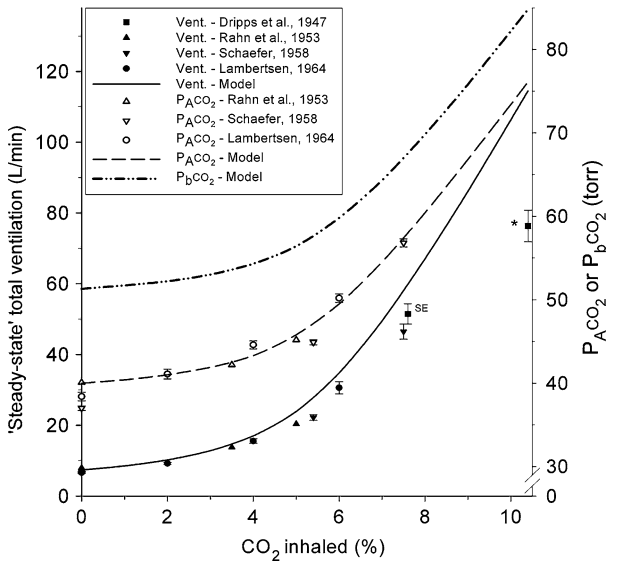

FIGURE 1. Shown are steady-state total ventilation and alveolar (A) P_{CO_2} for various values of inhaled %CO_2. Experimental means for ventilation from four studies (see legend) are shown by solid symbols with SE bars and P_{ACO_2} means from three of these studies are shown by open symbols. Model predictions of ventilation and P_{ACO_2} are shown by solid and dashed lines, respectively. Predicted brain (b) P_{CO_2} is shown by the dash-dotted line. The * indicates that the data point was measured prior to attaining steady state.

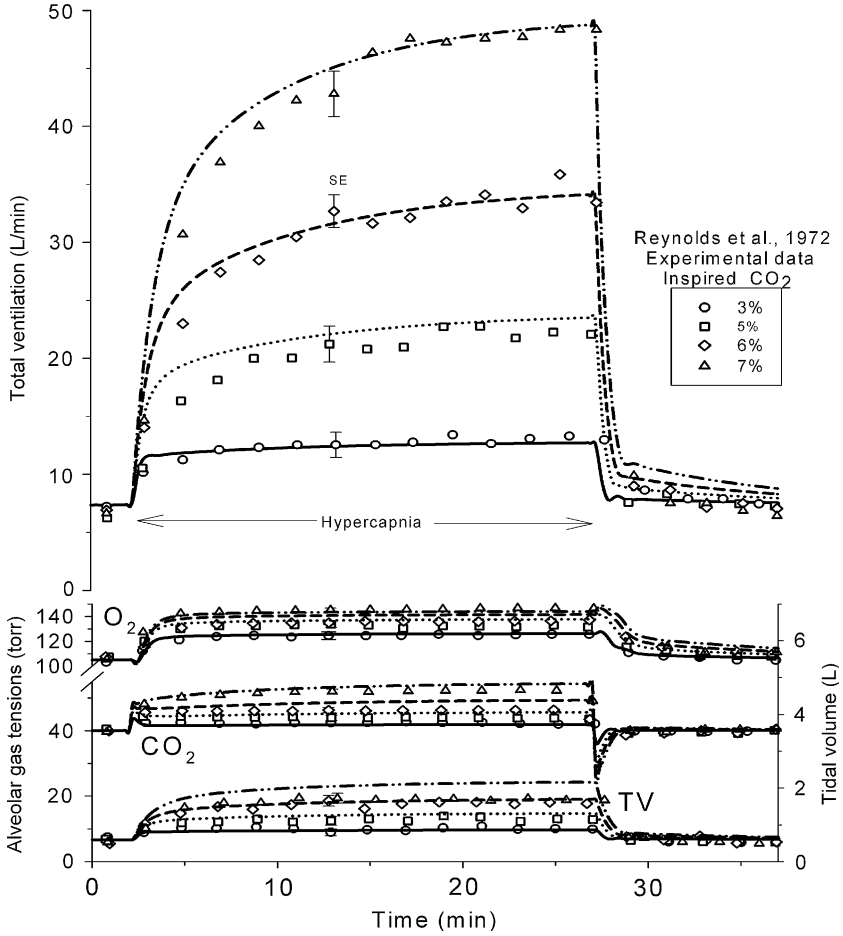

FIGURE 2. Measured total-ventilation transient responses (upper panel) due to inhalation of 3–7% CO_2 for 25 min from experiments by Reynolds *et al.*[37] are shown by the various open symbols with typical SE bars. Corresponding model predictions are shown by the various lines. The upper two sets of data in the lower pane are measured alveolar gas tensions produced by the CO_2 inhalation as indicated by the same open symbols as for ventilation. The corresponding lines show the model predictions. The lower set of data and curves are for measured and predicted tidal volumes.

magnitude of the average step from their steady-state ventilation values and a mathematical description of peripheral and central controller function devised by Bellville *et al*. For example, the predicted initial steady state P_{etCO_2} value for normal subjects was equal to their estimated P_{etCO_2} threshold of 36.5 torr plus the ratio of their steady-state ventilation of 7.5 L min^{-1} to their total controller gain of 2.13, the latter yielding a value of 3.5 torr, for a total of 40 torr. At the ventilation peak of 24.2 L min^{-1}, using the same procedure, the predicted value was 47.9 torr, giving a step of 7.9 torr, the value used in our model simulation (Fig. 3).

CO_2 Step Change in Euoxia with CB Resected

Simulation of CB resection was achieved by eliminating the ventilation induced by the peripheral chemoceptors and reducing the gain of the central chemoceptors; Bellville *et al.*[1] found that the gain of the central receptors was reduced to 52.5% of its normal value. However, these changes altered the steady-state ventilation and P_{ACO_2} values. We found that a change in the central threshold to 46.4 torr produced the ventilation of 7.03 L min^{-1} that matched the Bellville *et al.* data and yielded a P_{ACO_2} of 41.8 torr. These values were the initial, steady-state starting point upon which the step was imposed for the CB-resection simulation (Fig. 3).

Hypoxia during Eucapnia

Reynolds and Milhorn[36] measured transient changes in ventilation, alveolar-gas tensions, tidal volume, and respiratory rate for 10 min of 7, 8, and 9% O_2 inhalation with P_{etCO_2} clamped at normal values. Since these data were standardized as above, they were rescaled before comparison with model predictions. We simulated these experiments by having the model subject breathe each of these O_2 concentrations for

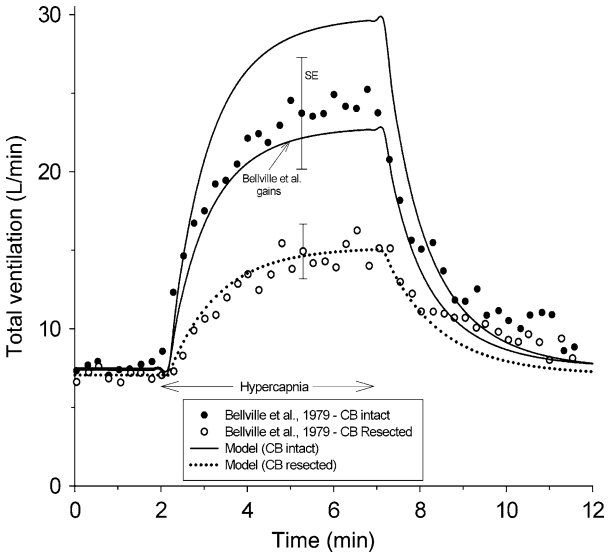

FIGURE 3. Measured total-ventilation transients with typical SE bars before, during and after a step change in end-tidal (et) P_{CO_2} are shown for two groups of subjects, those with carotid bodies (CB) intact (solid circles) and those with CB resected (open circles). Model predictions were determined for the intact case (solid lines) using a 7.9-torr step increase and for the resected case (dotted line) using an 8.4-torr increase. These step values were computed from the model given by Bellville *et al.*[1] and the average of the parameters estimated by them from their model. The model predictions shown by the upper solid line are using controller gains of Table 2. The predictions of the lower solid line are with controller gains of Bellville *et al.*

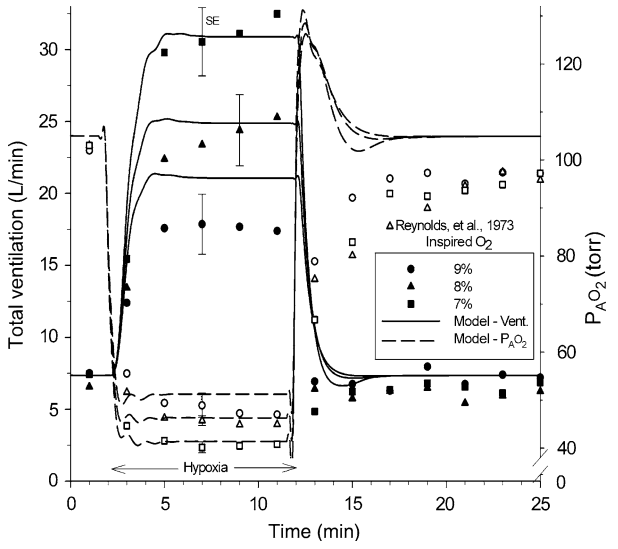

FIGURE 4. Total ventilation and alveolar-O_2 tensions before and after 10-min inhalations of 7, 8, or 9% O_2 at constant CO_2 (eucapnia) in experiments by Reynolds and Milhorn.[36] Solid and open symbols show measured ventilation and alveolar-O_2 values, respectively, for the three values of inhaled O_2. Corresponding model predictions are shown by solid and dashed lines, respectively.

10 min. Comparison of model predictions and experimental data were as in section "CO_2-Inhalation (Hypercapnia)" (Fig. 4).

Step Increase in P_{etCO_2} during Hypoxia

Bellville *et al.*[1] clamped P_{etO_2} at 53 torr and imposed a hypercapnic step for 5 min. They measured ventilation and end tidal gases as before. In order to match their initial ventilation of 7.63 L min^{-1} under the hypoxic conditions in the model, it was necessary to reduce our initial model P_{ACO_2} to 37.4 torr. The magnitude of the hypercapnic step was computed to be 11 torr using the data of Bellville *et al.* and the procedure described in section "End Tidal (et) CO_2 Step Increase" (Fig. 5).

Hypoxia followed by Hyperoxia during Poikilocapnia

Georgopoulos *et al.*[15] measured ventilation and gas tensions during a 35 to 51-s period of 8.5%-O_2 breathing followed by 100%-O_2 breathing for 2 min in nine subjects. CO_2 was allowed to freely vary (poikilocapnia). Their objective was to investigate the neural afterdischarge phenomenon (see Discussion). Experimental data were given at 5-s increments for a total of 45 s. We simulated this procedure by having the model subject breathe 8.5% O_2 for the first 45 s and 100% O_2 for the following 120 s (Fig. 6).

Poikilocapnic Hypoxia

Reynolds and Milhorn[36] used the same protocol and measurements as in Section "Hypoxia during

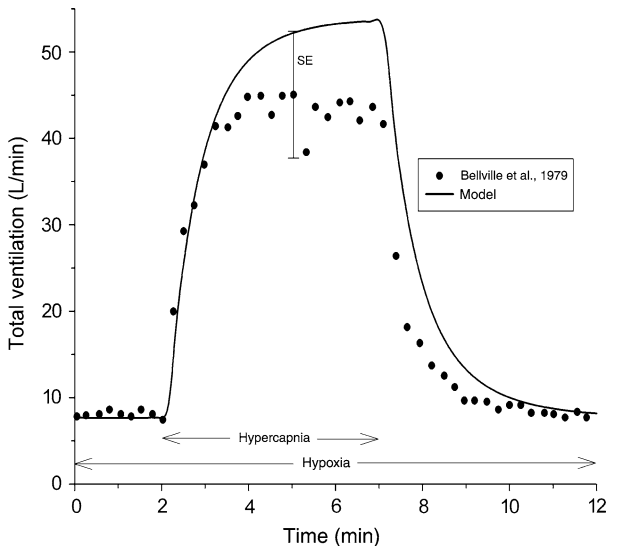

FIGURE 5. Measured total-ventilation transients (solid circles) from Bellville *et al.*[1] due to a step change in end-tidal P_{etCO_2} against a background of hypoxia ($P_{AO_2} = 53$ torr) are shown. Model predictions (solid line) were determined using an 11-torr step increase.

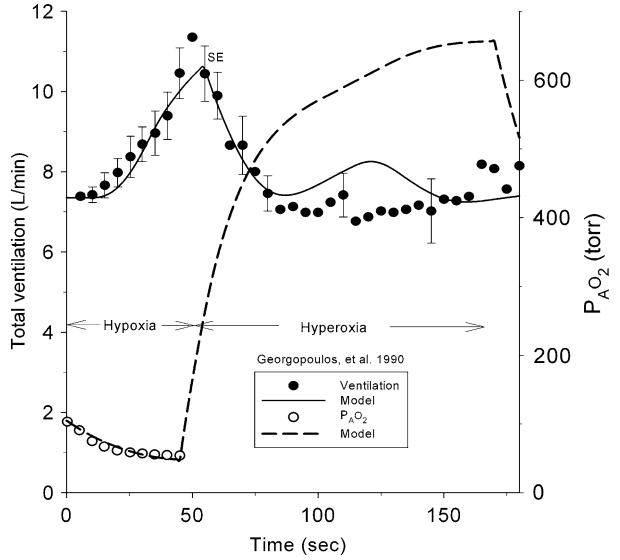

FIGURE 6. Measured transient ventilation data (solid circles) and alveolar P_{O_2} (open circles) from Georgopoulos *et al.*[15] are shown during a short phase of hypoxia ($P_{AO_2} = 55$ torr) followed by 100% O_2 breathing (hyperoxia). Corresponding model predictions are shown by the solid and dashed lines, respectively.

Eucapnia," except that CO_2 was uncontrolled. Their data were scaled as above and compared to model predictions (Fig. 7).

'Steady-state,' Inhalation of Gas Mixtures with Reduced O_2 with Varying CO_2 content

Nielsen and Smith[31] exposed two subjects to various concentrations of O_2–CO_2-containing gas mixtures, each for up to 30 min. The aim was to generate ventilation vs. P_{ACO_2} response curves at approximately fixed hypoxic P_{AO_2} levels. For just the lowest P_{AO_2} values to be attained by each subject, they gave the gas mixtures actually used to obtain data over the desired range of P_{ACO_2} values. We simulated their experiments by running the model for the same time periods they used with each gas mixture inhaled. (Fig. 8)

Hall[21] tried to achieve the same objective as Nielsen and Smith,[31] but with a different protocol. Subjects were brought to a simulated altitude of 22-K ft while breathing 100% O_2. They then breathed a succession of gas mixtures of 21% O_2 and increasing CO_2 concentrations up to 12%. Each gas mixture was breathed for 6 min and then the subject breathed 100% O_2 for the seventh min. Measurements were made of ventilation and P_{ACO_2} during the sixth min for each gas mixture. We simulated this protocol in our model experiments (Fig. 9).

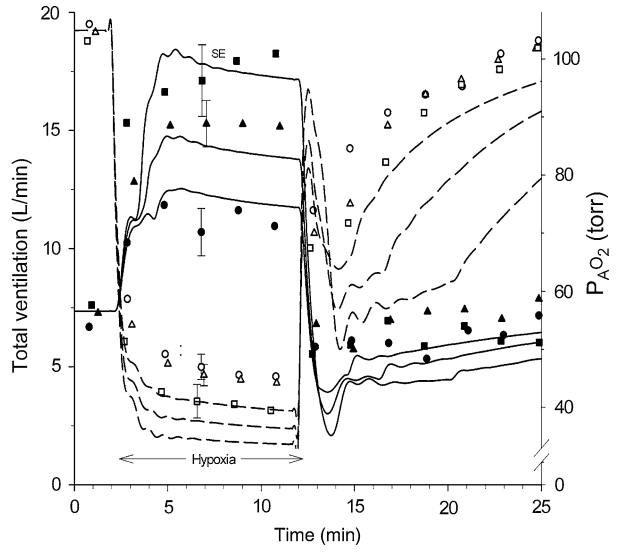

FIGURE 7. Total-ventilation and alveolar-O_2 data before and after a 10-min inhalation of 7, 8, or 9% O_2 with freely variable CO_2 (poikilocapnia) in experiments by Reynolds and Milhorn.[36] Symbols and lines are as in Fig. 4. Note that the response is much more oscillatory than when CO_2 was held constant (see Fig. 4).

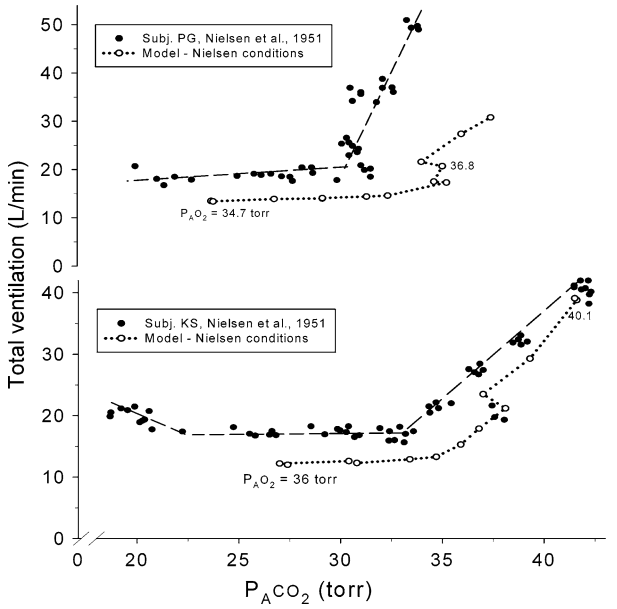

FIGURE 8. Measured 'steady-state' total ventilation plotted against P_{ACO_2} (solid circles) from Nielsen and Smith[31] experiments on two subjects. Starting with a hypoxic gas with no CO_2, subjects were exposed in 25–30 min sequences to gas mixtures of decreasing O_2 and increasing CO_2 to generate the experimental data at approximately constant P_{AO_2} of 36.9 torr (Subj. PG) and 39.2 torr (Subj. KS). The dashed lines, drawn by Nielsen and Smith suggest respiratory thresholds at a P_{ACO_2} of ~31–32 torr. The open circles connected by dotted lines show the model predictions using the same gas mixtures as Nielsen and Smith for the same lengths of time as their experiments. The numbers next to some points are the model P_{AO_2} values achieved using their conditions. The jaggedness in the latter curves is due the range of variation in predicted P_{AO_2} values. If P_{AO_2} were held absolutely constant, the curves would be continuous as described by Eqs. (10) and (11) and shown in Fig. 14. Because of the flatness of the predicted curves at lower P_{ACO_2} values and the steepness at higher values, it is possible to imagine a discontinuity at ~35 torr that could be interpreted as a respiratory controller threshold.

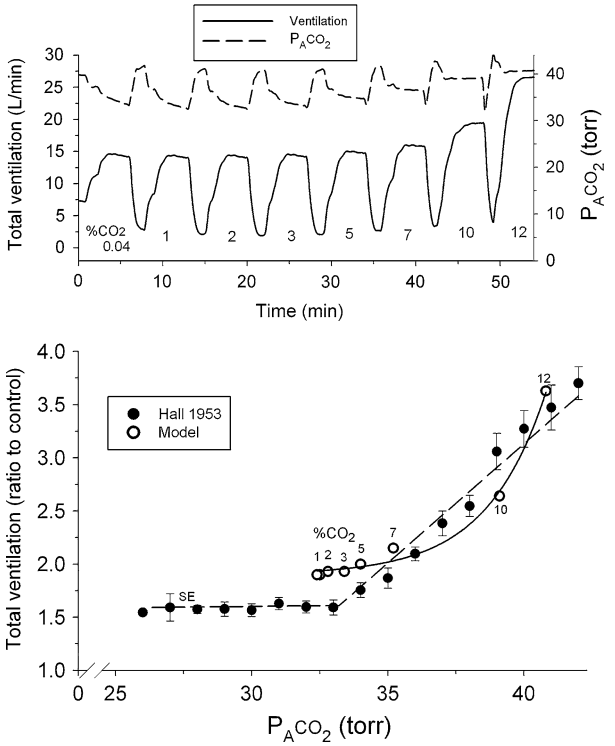

FIGURE 9. Shown in the upper pane are predicted transient changes in total ventilation (solid line) and P_{ACO_2} (dashed line) using the experimental protocol of Hall.[21] At a simulated altitude of 22-K ft, each section of the traces is a response to first 100% O_2 for 1 min (shown by the steep drop in ventilation) and then 5 min under ambient O_2 with increasing %CO_2 inhaled (% shown at bottom). The result is a sharp increase in ventilation and drop in P_{CO_2} followed by 'plateaus' ('apparent' steady state) in each variable. Shown in the lower pane are the experimental data (solid circles) of Hall[21] using the protocol above. The intersection of the two dashed lines drawn through the data suggests a ventilatory threshold at about 33 torr. The open circles represent the 'plateau' values of ventilation plotted against 'plateau' values of P_{ACO_2} from the simulation data above for each %CO_2 inhaled (number next to point). The solid line is a curve fit to the latter data. The intersection of tangents (~37 torr) that could be drawn to the groups of predicted data at low and high P_{ACO_2} values could be viewed as suggestive of a controller threshold just as in Fig. 8.

Experiments at Altitude

Rahn and Otis[34] measured steady-state alveolar gas tensions in men exposed to various simulated altitudes in a low-pressure chamber, but for just 1-h periods to avoid acclimatization effects. We simulated this condition by running the model for 60 min at their simulated altitudes (Fig. 10).

Respiratory Model Predictions at Altitude

We explored the effects on ventilation of a simulated altitude-chamber experiment where the subject was exposed to a sequence of altitudes while changing gas mixtures between ambient air and 100% O_2 (Fig. 11).

The effect on ventilation of a rapid decompression in a commercial aircraft was explored by decompressing from the 8-K ft pressurized cabin altitude to 40-K ft in 60 s, a 10-s stay at that altitude and then a slowed descent back to 10-K ft. This maneuver was accomplished without and with supplemental O_2 (Fig. 12).

The effect of the time required to don the O_2 mask was determined by extending this time out from 0 to 60 s. Supplemental O_2 was available through the mask above 14.4-K ft as in present commercial aircraft (Fig. 13).

Generation of Steady-state Controller Curves

We generated model predictions of steady-state ventilation at various fixed values of P_{AO_2} as P_{ACO_2} was varied over a wide range. These controller curves were compared to the predictions of an equation proposed by Severinghaus.[41] We also generated such curves when P_{ACO_2} was held at fixed values and P_{AO_2} was varied over a wide range (Fig. 14).

Curve-fitting and Simulation Procedures

Experimental data were fit with linear and nonlinear curves using either SigmaPlot or Tablecurve 2D (SYSTAT Software, Richmond, CA). The model equations were simulated using VisSim (Visual Solutions, Inc., Westford, MA) version 6.0. The integration algorithm was Runge Kutta 4 with a time step of 0.01–0.02 s. The running speed was 10 to 20-times real time using a Pentium (R) 2.8 GHz processor.

RESULTS

Model Validation

Steady-state

We ran the model for 60 min under sea-level conditions to assure solution stability. After an initial transient of < 5 min due to time delays in the system, values of all the variables remained constant for the remainder of the run. Table 1 gives the variables of interest, their units, and their steady-state values for our normal, awake, resting human. Also shown are model predictions from Grodins *et al.*[18] They formulated two versions of their model so we reported the results of both of these. For the most part, we used their parameter values (see Table 2), hence, it is not surprising that most of the steady-state values of the variables are quite similar between the two studies. However, since there were some major differences between plant and controller formulations as described above, it is also not surprising that there are differences

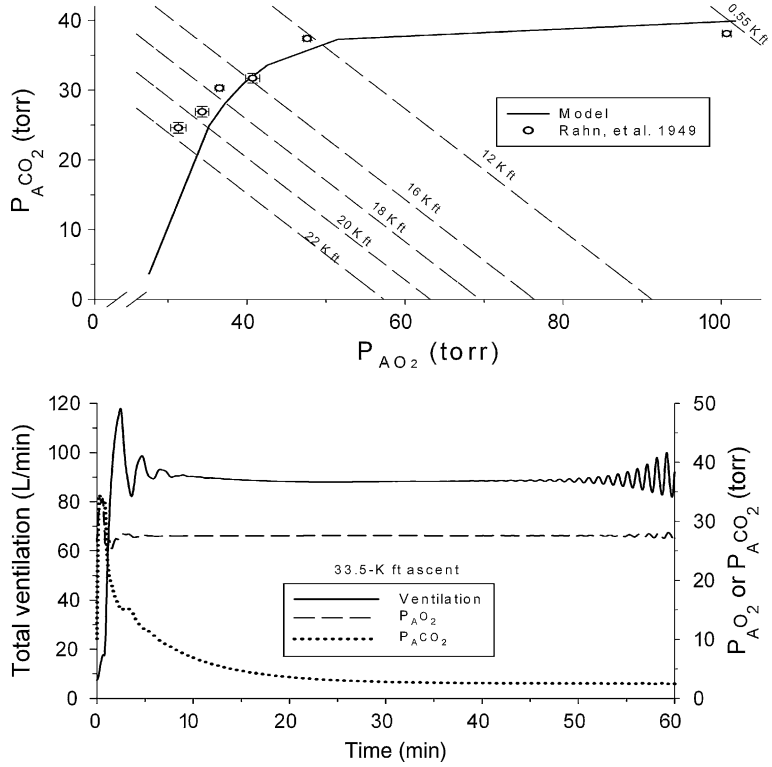

FIGURE 10. Alveolar gas tension measurements from Rahn and Otis[34] for unacclimatized subjects exposed to various simulated altitudes are shown by open circles (upper pane). Dashed lines show lines of constant altitude. The solid line shows the model predictions. Model predictions of ventilation (solid line) and alveolar gas tensions at a simulated altitude of 33.5-K ft are shown in the lower pane. Note that a spontaneous unstable oscillation begins about 40 min after the altitude exposure.

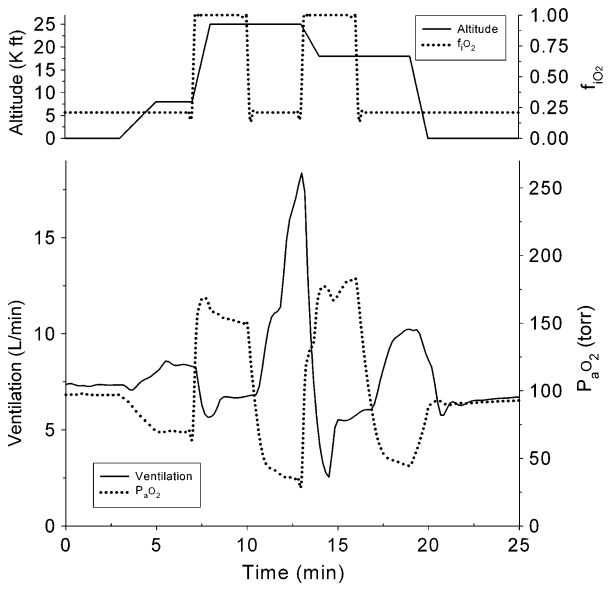

FIGURE 11. Simulation of an altitude-chamber, hypoxia-training exercise. Shown in the bottom pane are predicted changes in ventilation and P_{AO_2} (solid and dotted lines, respectively) as altitude (upper panel, solid line) is increased from sea level to 25-K ft and then returned in steps to sea level. The subject is breathing either ambient air or 100% O_2 as indicated (upper panel, dotted line) by the changes in the fraction (*f*) of inspired gas that is O_2.

in the variable values between the studies, notably in brain and tissue. As seen in Table 2, O_2 gas tensions in brain and tissue in the present model are a few torr lower and CO_2 tensions are a few torr higher than in the Grodins *et al*. model.

All fundamental parameter values from Table 2 were unchanged during the following phases of this study, except where noted.

Hypercapnic Steady state

There are a number of studies that have subjected humans to the inhalation of gas mixtures with various concentrations of CO_2 and measured steady-state changes in total ventilation and P_{ACO_2}. Figure 1 illustrates four sets of ventilation data attained (solid symbols with SE bars) and corresponding P_{ACO_2} values (three studies, open symbols) for various percentages of inspired CO_2 compared to corresponding model predictions (solid and dashed lines, respectively). As seen, other than at the highest $\%CO_2$ inhalation, the model predicts these steady-state data quite closely. In the experiments at very high $\%CO_2$ inhalation, it was likely that steady state was not attained. This conclusion was affirmed by Grodins *et al.*[18] and is evident in our model transient predictions (see Fig. 2). These

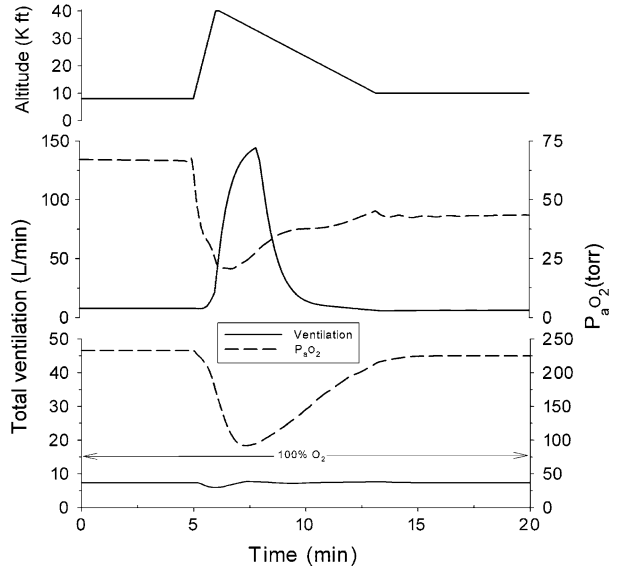

FIGURE 12. Prediction of ventilation and P_{aO_2} responses (solid and dashed lines, respectively, in the lower two panes) to rapid decompression to 40- K ft from 8-K ft (altitude in upper pane) and then gradual descent back to 10-K ft. The subject is breathing ambient air in the middle pane and 100% O_2 in the lower pane.

results show that the form and parameters chosen for the CO_2 part of the controller (Eqs. 9 and 10) are adequate to closely describe the experimental responses. Also shown is the predicted brain tissue CO_2 (P_{bCO_2}) values (dash-dotted line). Steady-state P_{bCO_2} is greater than P_{ACO_2}, but the difference diminishes at higher CO_2 values. The two variables are

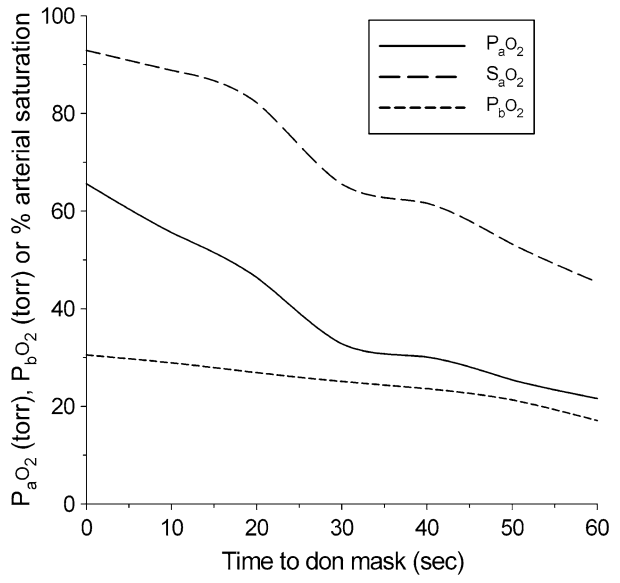

FIGURE 13. Decrease in minimum P_{aO_2}, P_{bO_2} and O_2 saturation reached before donning mask as a function of time required to don mask.

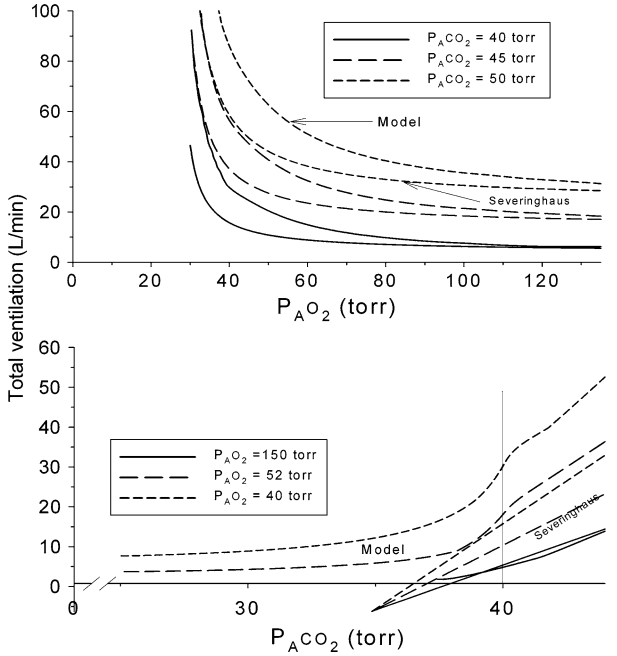

FIGURE 14. Model-predicted respiratory-controller ventilation curves at constant values of P_{ACO_2} (upper pane) and P_{AO_2} (lower pane), respectively, are shown by solid, dashed and dotted curves. The predicted curves in the lower pane show the characteristic 'dog-leg' shape and form part of an Oxford-fan-like family of curves. Also shown in each panel are the predictions by the equation of Severinghaus[41] using the corresponding gas tension values as above. In the upper panel, the Severinghaus-predicted curves have the same shape as our model predictions, but are displaced below the latter. In the lower panel, the Severinghaus predictions are a family of straight lines intersecting at a negative ventilation point.

related by the empirical equation $Y = -15.34 + 1.082^{*}X$, where Y and X stand for P_{ACO_2} and P_{bCO_2}, respectively. This relation is useful if one wants to cast steady-state controller equations in terms of alveolar (blood)-gas concentrations.

Transient Hypercapnia

The data measured by Reynolds *et al.*[37] during hypercapnia allow for a more complete test of the model because of the range of CO_2 inhalations used, the number of variables measured and their measurement of transient changes. The upper set of curves in Fig. 2 shows the comparison between model predictions of ventilation (solid, dashed, and dotted lines) and experimentally measured changes (open symbols). Selection of the values of the two gains and thresholds of the controller set the maximum ventilation value for the 7% O_2 inhalation curve (uppermost). As seen from the typical SE bars on each curve, the predictions are excellent for transient changes and steady-state values for all curves. In the lower section, are shown the changes in O_2 and CO_2 alveolar-gas tensions (two uppermost curves) and tidal volume (lowest curve) due

TABLE 2. Model parameters.

Parameter	Units	Value	
		Present study	Grodins *et al.*[18]
MR_tO_2	L min^{-1} (STPD)	0.215	0.215
MR_bO_2	L min^{-1} (STPD)	0.05	0.05
MR_tCO_2	L min^{-1} (STPD)	0.182	0.182
MR_bCO_2	L min^{-1} (STPD)	0.05	0.05
RQ_t		0.875	0.875
RQ_b		1.00	1.00
f_{shunt}		0.015	
V_t	L	40	39
V_b	L	1	1
T_bCO_2	torr	48.4	
$T_{cb}CO_2$	torr	38.7	
K_bCO_2	L min^{-1} torr^{-1}	2.08	
$K_{cb}CO_2$	L min^{-1} torr^{-1}	1.04	

to the hypercapnia. As seen, the model predicts these families of data with good accuracy. These results give confidence into the validity of the respiratory plant and controller structures relative to CO_2 dynamics.

CO_2 Step Increase

We sought further validation of the CO_2-related structure of the model by using the data of Bellville *et al.*[1] These investigators devised a method of clamping end-tidal (et) CO_2 tension to achieve a step increase. Their measured ventilation response to such a step maintained for 5 min is shown in Fig. 3 (solid circles). The model predictions (upper solid line) somewhat overestimate the mean experimental values at the various time points, but the SE range is quite broad as shown by the typical SE bars. Bellville *et al.* estimated gains of the peripheral and central controllers from their experimental data. If we use their gains in the model, the predictions are much closer (lower solid line). This discrepancy highlights the difficulty of accurate model prediction. If the model parameters are optimized to closely fit one set of experimental data, the predictions may be less close for another data set.

Hypercapnia with CB Resection

Also shown in Fig. 3 is the experimental ventilation response (open circles) and corresponding model-predicted response (dotted line) for subjects with resected carotid bodies.[1] This resection was simulated by clamping $\dot{V}_p$ to zero and using the reduced central chemoceptor gain estimated for these subjects. Hence, changing only one parameter value allowed accurate prediction of transient and steady-state responses.

Hypoxia during Eucapnia (Normocapnia)

Experimental data in the literature for hypoxia combine this forcing with various manipulations of P_{CO_2}, fixed, either eucapnic or hypercapnic, or poikilocapnic (freely variable CO_2). Hypoxia is usually attained by breathing gas mixtures with low concentrations of O_2.

The most complete data set for eucapnic hypoxia is by Reynolds and Milhorn.[36] They subjected individuals to inspired O_2 concentrations of 7, 8, and 9% for 10 min and measured ventilation and alveolar-gas concentrations. Figure 4 shows the changes in total ventilation (solid symbols) and alveolar O_2 tension (open symbols) and the comparisons to the corresponding model predictions, solid and dashed lines, respectively. The parameters of the hyperbolic part of Eq. (10) were chosen to match the steady-state ventilation predicted by the model to the approximate steady-state of the experimental data for the 7%-O_2 inhalation (solid squares). The resulting predictions for the other two O_2-inhalation curves are slightly overestimated. The minimum P_{AO_2} values achieved during the hypoxic phase were quite closely predicted by the model, but instead of the undershoot and slow return to initial baseline shown by the experimental data, the model predicted an overshoot and a much quicker return to initial baseline values.

Step Increase in P_{etCO_2} during Hypoxia

In the same study as in section "CO_2 Step Increase," Bellville *et al.*[1] measured changes in ventilation due to a step in P_{etCO_2} induced upon a background of hypoxia. Figure 5 shows the resulting changes in ventilation. As seen, the model predictions slightly overestimate the increase in ventilation, but the SE bars for the experimental data are quite large. The ability of the model to predict these ventilation data with acceptable accuracy stemmed from the functional form of Eq. (11) under hypercapnic conditions.

Hypoxia Followed by Hyperoxia during Poikilocapnia (Freely-variable CO_2)

Data from a study by Georgopoulos *et al.*[15] provided validation for model ventilatory-control dynamics. Figure 6 shows the results. As seen, the model transient ventilation predictions (solid line) in the hypoxic phase closely follow the measured increases (solid circles). Predicted ventilation shows some oscillation upon cessation of hypoxia and introduction of hyperoxia, but is basically similar to the experimental changes. These oscillatory dynamics depend upon the value of the time constant in the peripheral chemoceptor loop. Ventilatory oscillations resulting from hypoxia have been produced in simulations by a number of other investigators.[18,25,30,46,48]

Poikilocapnic Hypoxia

The study by Reynolds and Milhorn[36] in section "Hypoxia during Eucapnia (Normocapnia)," also included experiments where hypoxia was induced, but CO_2 was allowed to vary. Figure 7 shows the changes in ventilation and alveolar P_{O_2} under these conditions. The form of Eq. (11) was determined to have the model ventilation predictions during hypocapnia approximately match experimental ventilation data over the ~6–12 min time period. As seen, predictions were usually within the variability indicated by the SE bars. Predicted ventilation data following the step showed an undershoot not seen in the experimental data, but the 2-min gap between experimental data points may have masked this response. The oscillations shown on the predicted-ventilation curves were much more evident than in Fig. 4 where P_{ACO_2} was held constant. The curves became more oscillatory as P_{ACO_2} was reduced. P_{AO_2} predictions were a few torr lower than those measured during this hypoxic phase. Removal of the hypoxic stimulus produced an oscillatory predicted-P_{AO_2} response that was slow to return to pre-hypoxic levels, particularly for the 7%-O_2 inhalation condition. These dynamics were not evident in the measured responses. The minimum P_{ACO_2} values attained at the end of hypoxia were within about 1 torr of the experimental minimums (not shown).

Steady-state Ventilation vs. P_{CO_2} Curves during Hypoxia

The ventilation data (filled circles) for a range of alveolar P_{CO_2} at constant P_{ACO_2} for two subjects as measured by Nielsen and Smith[31] are shown in the upper and lower panes of Fig. 8. Nielsen and Smith drew asymptotes through these data (dashed lines). The inflection points at the knee (~32–34 torr) of each curve were suggested as threshold points for the central respiratory controller. The model results (open circles and connecting dotted lines) were determined from the $\%O_2$ and $\%CO_2$ inhalations and the exposure times given by them.[31] The numbers next to some points show the range of predicted P_{AO_2} values attained at the end of the measurement period. As seen, the model predicts a similar pattern of a transition from an almost flat slope to a much increased slope, but the transition region is a few torr higher than drawn for the experimental data. The predictions would show a smooth transition, characteristic of the function of Eq. (11), if P_{AO_2} was constant. However as seen, the conditions used by Nielsen and Smith resulted in steady-state P_{AO_2} values that varied over a range of 2–4 torr for the subjects.

Hall[21] wanted to further investigate the apparent threshold found by Nielsen and Smith[31] using a somewhat different protocol. As seen in the upper pane of Fig. 9, a series of periods of inhalation of increasing concentrations of CO_2 imposed on a background of hypoxia produced a series of transient changes in ventilation and alveolar P_{CO_2}. Although Hall claimed that both of these variables were at steady state at the end of each inhalation period, it is clear they are still decreasing at inhalations less than about 7%. The bottom pane of Fig. 9 shows the comparison of experimental results (solid circles and dashed line fit of Hall) and model predictions (open circles) taken from the upper pane. The $\%CO_2$ inhaled is shown next to each point. Because of the variability of individual subject responses, the experimental P_{ACO_2} values achieved ranged down to 26 torr and appear continuous to beyond 40 torr. There appears to be an inflection point at about 33 torr. In contrast, the minimum model P_{ACO_2} was 32 torr and there are a discrete number of data points corresponding to the seven different concentrations of CO_2 inhaled. The curve through the predicted data is smooth, with no inflection point. However, a tangent line drawn through the lower P_{CO_2} set of points and another one through the upper two would intersect at about 38 torr, thus suggesting such a threshold point.

Experiments at Altitude (Low-pressure Chamber)

Figure 10 (upper pane) shows the measured alveolar-gas tensions (open circles) of Rahn and Otis[34] who exposed subjects to 60 min of altitude-induced hypoxia in an altitude chamber. The experimental data are for simulated altitudes of 0.55 to 22-K ft (dashed lines). The solid line shows model predictions extended to an altitude of 33.5 K ft. As seen, the predictions are within a few torr of the experimental data. As seen in the lower pane, the predicted ventilation and other variables broke into a spontaneous, unstable oscillation about 40 min after exposure to the 33.5-K ft altitude. This oscillation is likely due to the high controller gain at this extreme level of hypoxia. It was not due to a numerical instability as reducing the integration time-step did not eliminate it.

Rahn and Otis[34] used their gas tension data to predict the changes in alveolar ventilation at each simulated altitude. Table 3 (column 2) shows these results. The alveolar ventilation data were calculated from

$$\dot{V}_A = 0.864 \times \frac{MR_{O_2} \times RQ}{P_{ACO_2}} \qquad (14)$$

where MR_{O_2} is the rate of O_2 utilization in mL min^{-1} and RQ is the respiratory quotient. Rahn and Otis assumed a constant rate of O_2 utilization at all altitudes so this term cancelled out in the calculation of

TABLE 3. Predictions of calculated alveolar ventilation changes at altitude by Rahn and Otis.[34]

Altitude (K ft)	Rahn *et al.* calculated	Model
0.55	1	1
16	1.31	1.26
18	1.43	1.43
20	1.62	1.65
22	1.81	1.95

ventilation ratios. They also assumed an average RQ of 0.82 for all their calculations. Column 3 of the Table shows the predictions of the model. As seen, they are close to the experimental estimates.

Model Predictions at Altitude

Changes in ventilation (solid line) and arterial P_{O_2} (dotted line) as a result of exposure to altitude, either breathing ambient air or 100% O_2 through a mask during a simulated altitude-training exercise, are shown in the lower pane of Fig. 11. The upper pane shows the altitude (solid line) sequence changes and the periods of ambient or 100% O_2 breathing (dotted line). As seen, between min 7 and 10, exposure to 25-K ft altitude while breathing 100% O_2, does not stimulate an increase in ventilation because P_{O_2} is not in the hypoxic region. However, when the mask is removed and P_{O_2} drops, there is a rapid increase in ventilation to almost 20 L min^{-1}. During this hypoxic phase, arterial P_{O_2} falls to low levels, about 35 torr. At this point, arterial-hemoglobin O_2 saturation (not shown) is close to 70%. Sustained exposure to such low levels, without the use of supplemental O_2, can induce syncope in unacclimatized individuals.[22,23] Hence, supplemental O_2 is mandatory at this altitude for crew and passengers in commercial aircraft. A similar scenario, but less severe, occurs upon removing the mask at 18-K ft (min 16–18).

A rapid decompression to 40-K ft is a significantly more dangerous situation than the exercise above. Figure 12 shows the respiratory responses to a decompression from 8-K ft (normal airline cabin pressure) to 40-K ft in 1 min and then the gradual descent back to 10-K ft. The upper pane shows the timing of the altitude changes. The middle and lower panes show the responses without and with supplemental O_2, respectively. As seen in the middle pane, the decompression results in a rapid fall in arterial P_{O_2} that stimulates maximal ventilation. Ventilation returns towards normal after P_{O_2} rises during descent. It is likely that syncope would have occurred at some point during the fall in P_{O_2}, however, nothing in the present simulation predicts this event or changes respiratory behavior as a result. In the bottom pane, the exposure to 100% O_2 for the entire time of decompression avoids any significant ventilatory changes as P_{O_2} never drops to a hypoxic level.

The model can be used to explore the effect of the lag time in donning the O_2 mask. We assumed that at 14.4-K ft, these masks automatically descend from the ceiling and O_2 is flowing. Figure 13 shows these results. Shown are the decreases in arterial saturation (long-dash line), P_{aO_2} (solid line), and brain PO_2 (short-dash line) as the time to don the mask increases. Using any of these measures, it is clear that extending this time significantly increases the chance of syncope occurring.

DISCUSSION

The aim of this study was to use mathematical simulation to explore the predictions of a model of human respiration in the awake state that could be used to understand the respiratory responses of individuals exposed to high altitudes for short periods of time. The results of this exercise could give considerable insight into the respiratory responses induced by the potentially dangerous hypoxia at altitude, a situation not easily studied experimentally. In this initial investigation, we found that a typical training session, where simulated altitudes as high as 25-K ft are encountered, when sustained, is capable of producing hypoxia (Fig. 11) that would likely result in syncope.[23] In a rapid decompression to 40-K ft, supplemental O_2 is absolutely required to avoid a similar scenario (Fig. 12). If the O_2 mask is not donned in sufficient time (Fig. 13), then O_2 levels in the body could again reach critically low levels. Although these qualitative conclusions have been reached before by the aviation community, the model now yields quantitative predictions which can give more weight to their validity. A very important outcome of this study is that this well-validated model can be used to predict responses of subjects using newly developed O_2 masks and O_2-delivery systems being proposed for use in various aircraft.

Of course, confidence in the predictive ability of a model is only as good as the breadth and depth of the experimental data against which it is validated. In the present study, we have tried to compare model predictions to almost all the appropriate data known to us for pure hypercapnic conditions and for the wide range of short-term (< 10 min) hypoxic conditions, uncoupled and coupled with hypercapnia and hypocapnia. Data intentionally excluded were those for longer-term hypoxia where the HVD phenomenon was prominent (see below). As seen in our extensive validation (Figs. 1–10), for the most part, the model predictions of ventilation and O_2 and CO_2 gas tensions were quite

close to the experimental data, both transient and in the steady-state. The model predicts many more variables, but most of these have not been measured or cannot be measured with present technology.

Important in the present model is its ability to describe the changes in ventilation produced by changes in CO_2, both greatly increased and decreased from normal, at normal and hypoxic levels of PO_2. Historically, in the awake state, such respiratory controller descriptions have been characterized by a family of curves, variously referred to as 'dog-leg' or 'hockey-stick' shaped,[6] or also described as the 'Oxford fan', [20] particularly in the hypercapnic region. This family is typically displayed as a series of straight lines converging to a single point as shown in the lower panel of Fig. 14. This description is from Severinghaus[41] who suggested these lines as typical experimental responses to increases in CO_2 while alveolar P_{O_2} is held constant at hypoxic levels. As seen, the lines predict that ventilation is driven to zero at P_{CO_2} values < 36–38 torr depending upon P_{O_2} levels. This type of formulation may be appropriate under sleep conditions where apnea can be produced, but it is not applicable to awake humans under conditions of severe hypocapnia seen at high altitude (see Fig. 10). In contrast, our model predictions under hypocapnic conditions show that ventilation changes become almost insensitive to variations in P_{CO_2} under these conditions. This behavior resembles the measured data of Nielsen and Smith[31] shown in Fig. 8 and Hall[21] in Fig. 9. As seen, our model predictions only become linear at P_{CO_2} values a few torr above the normal value of 40 torr and then continue on to form the characteristic fan-like form for the various constant PO_2 values. This behavior is due to the different formulations we used (Eq. 11) for the conditions of hypercapnia and hypocapnia. The predictions are continuous at the 40-torr point, but the change between the two functional forms produces an inflection point that may not be real. Therefore, our model predictions do not indicate a respiratory controller threshold as suggested by the measurements of Neilsen and Smith and Hall, even though such thresholds exist in our controller formulation. Whether or not such a threshold can be determined from respiratory data in awake humans is controversial.[7] Duffin *et al.*[11] has unmasked such thresholds using rebreathing experiments. However, Patrick *et al.*[32] confirmed our results in that they did not see a threshold-like inflection point in hypocapnic-induced respiratory responses in awake humans.

Another approach to characterizing these controller curves is shown in the upper panel of Fig. 14. Cormack *et al.*[4] measured changes in ventilation as P_{O_2} was varied, but P_{CO_2} was kept constant at normal or hypercapnic levels. Hence, their results are not applicable to hypocania, our major interest. Their experimental data had a hyperbolic shape as shown qualitatively by both our model's prediction and the equation of Severinghaus.[41] As expected from the results in the lower pane, the predictions of our model and that of Severinghaus[41] diverge as P_{O_2} is reduced. We did not try to compare these predictions with the data of Cormack *et al.* because of the large variability of the latter.

It was necessary to make some fundamental assumptions about the respiratory controller in the present simulation. These assumptions have many similarities to those of an early study by Duffin *et al.*[10] and to more recent studies,[30,46–48] but also some major differences. The assumptions are: (1) the controller is composed of two separate sets of chemoceptors, central and peripheral, whose ventilation signals add to achieve the total ventilation signal. (2) The central controller produces a ventilation signal which is a linear function of brain CO_2 and has a threshold below which the signal is zero. This threshold value is below the model's resting P_{bCO_2} so that the central signal contributes to resting ventilation (see Eq. (9) and Tables 1 and 2). (3) The peripheral chemoceptor response includes a linear function of CO_2 that contributes to resting ventilation and a nonlinear term expressing the interaction of CO_2 and O_2 on ventilation (Eq. 10). Equation (9) and the linear part of Eq. (10) set resting ventilation. (4) The O_2 contribution to ventilation is given by the hyperbolic relationship of Eq. (10) with parameter values selected to have model predictions approximate the experimental steady-state ventilation increases due to eucapnic hypoxia (see Fig. 4). (5) We assumed a multiplicative effect of CO_2 on the hypoxic ventilation drive (Eq. 10). The form of the CO_2 effect during hypocapnic-hypoxia is a function of the inverse of the ratio of P_{aCO_2} to its resting value raised to the fourth power. This form allowed predictions to approximately match the steady-state hypoxic experimental data of Fig. 7. The form during hypercapnic-hypoxia was this ratio raised to the third power. The ability to approximately match the hypercapnic-hypoxic experimental data (Fig. 3) of Bellville *et al.*[1] was dependent upon this latter functional form. At this time, we know of no mechanism producing the shapes of these curves (see Fig. 14), however, it is clear that the existence of controller thresholds do not produce noticeable discontinuities in these curves.

Our controller formulation differs from those of recent studies in a number of ways. Ursino *et al.*[47] used a constant resting ventilation value as did the original Grodins[18] model; the shape of their curve relating peripherally induced ventilation to P_{O_2} is sigmoidal; hypoxic ventilatory response is modified by a logarithmic function of P_{CO_2}; ventilation is not allowed to become negative during strong ventilatory inhibition of

control functions, but it could go to zero. Longobardo *et al.*[30] assumed that the chemical controller was defined in two regions separated by a 'transition' P_{CO_2} threshold; controller gains are higher above this threshold and lower below it; total ventilation is the sum of the chemical drive, alertness drive of the individual and other neurally mediated drives (see below); the hypoxia drive is a linear function of O_2 saturation. The Longobardo controller has the potential of describing ventilation changes during hypocapnic hypoxia, but their only validation was qualitative. Topor *et al.*[46] used a quite different approach. They assumed that total ventilation is described by the formulation of Severinghaus;[41] their central controller formulation is a linear function of brain CO_2 and arterial CO_2 is derived from brain P_{bCO_2}. They subtracted the resulting formulation from that of total ventilation to derive the peripherally induced ventilation function; the central contribution can become negative and subtract from this peripheral contribution; total ventilation can go to zero to simulate conditions encountered during sleep.

The Ursino *et al.*[47,48] model was able to predict longer-term ventilation changes due to eucapnic and poikilocapnic hypoxia, however, for validation of poikilocapnic hypoxia, the major focus of the present study, they used the data of Easton *et al.*,[13] which actually was measured under eucapnic conditions. Our evaluation of their controller equations suggested that they could not yield the dog-leg shaped curves necessary to describe ventilation changes due to decreases in P_{CO_2} at constant P_{O_2} levels. The Longobardo *et al.*[30] model was designed primarily to investigate periodic breathing during sleep and other conditions. They simulated the dogleg-shaped controller curves by using different CO_2-response slopes above and below their CO_2-transition threshold. There were only qualitative comparisons of model predictions to experimental data. Topor *et al.*[46] validated their model by comparing predicted ventilation responses to a hypercapnic step under normoxic and hypoxic conditions using the data of Bellville *et al.*[1] as in the present study (Figs. 3 and 5). However, the experimental data shown for the normoxic, hypercapnic step was that of a CB-resected individual (open circles in Fig. 3) and the experimental data shown during hypoxia was for a normoxic, hypercapnic step (solid circles in Fig. 3). Because ventilation could be driven to zero at reduced P_{CO_2} values, the controller formulation is not appropriate for our present application.

Another important feature of recent models is their simulation of the effect of O_2 and CO_2 on cardiac output and cerebral blood flow. Ursino *et al.*[47] assumed that hypoxia increased both blood flows in an exponential manner. The additive effect of CO_2 on cerebral blood flow was taken from Reivich[35] as in the present study and CO_2 had no effect on cardiac output. No comparisons were made with experimental data. Longobardo *et al.*[30] assumed that cerebral blood flow changed linearly with CO_2 and had an additive effect inversely proportional to arterial O_2 saturation. However, the rationale for these assumptions was not given. Our simulation of the effects of O_2 and CO_2 on these blood flows generally followed the approach of Topor *et al.*[46] by fitting logistic-type functions to human data, but we found some data not used by them to be more appropriate and we question their use of four different time constants to describe on- and off-transients for hypercapnic- and hypoxic-effects on cerebral blood flow derived from experimental data of Poulin *et al.*[33] The estimated time constants by Poulin *et al.* were extremely variable for both the on- and off-transients of the hypoxic effects (0.2–165 s, for on-transients, for example). Only the 6.1 s time constant for the hypercapnic effect was statistically significant. Hence, we used a 6-s time constant for all cerebral blood flow changes. We also used the 15-s time constant to slow changes in cardiac output as suggested by Topor *et al.*[46] We used a multiplicative approach of simulating changes to these flows rather than their additive approach. These differences between the present model and these more recent ones likely yield differing predictions, but the quantitative importance of these differences is difficult to determine.

We simulated the phenomenon of short-term potentiation or neural afterdischarge by inserting a 35-s time constant in the peripheral chemoceptor loop. The resulting model transient predictions to a short hypoxia followed by hyperoxia (Fig. 6) were quite close to the experimental measurements under these conditions by Georgopoulis *et al.*[15] Hence, the dynamics of both hypoxia onset and cessation were accurately simulated. The Ursino *et al.*[48] model qualitatively predicted the experimental results of Geogopoulis *et al.*[15] Longobardo *et al.*[30] simulated only the post-hypoxic phase with a 15-s time constant. Topor *et al.*[46] used a 35-s time constant after ventilatory stimulus initiation and 18-s time constant for the response after removal of the stimulus. Topor *et al.*[46] referred to the Georgopoulis data and to other data for their time constant selection. Our survey of the available data did not compel the use of two different time constants.

All three recent models addressed the phenomenon that the ventilatory response to sustained hypoxia rapidly reaches some maximum value, decreases slowly to about half this value over the next ~30 min and then returns to the initial maximum over the next 30–60 min. This phenomenon has been variously referred to as hypoxic ventilatory decline or depression (HVD). The predictions of the Topor *et al.*[46] model that simulated only the hypoxia-induced cerebral blood flow

changes suggested that about half of this slow initial decrease is caused by hypoxia-induced changes in cerebral blood flow, whereas the other half could be induced by a central inhibitory mechanism. Ursino *et al.*[47,30] simulated HVD by slowly inhibiting the gain of the peripheral chemoceptors in a nonlinear manner. In the present model, we did not specifically simulate this phenomenon for a number of reasons. (1) The short-term hypoxic data we used for comparison to model predictions did not show this decrease in ventilation (see Figs. 4 and 6), (2) the centrally induced component does not play a significant role in the short-term hypoxia investigated in the present study, and (3) the dynamics of the HVD effect varies significantly across the various experimental studies. It should be noted that even though we simulated the effect of hypoxia on cerebral blood flow, we did not see much of a ventilatory overshoot on the ventilatory response (see Figs. 4 and 6).

Missing from the present model is a simulation of CO_2 exchange between the brain and cerebrospinal fluid (CSF) as included by Grodins *et al.*[18] Using their constants, we found that the small amount of exchange that occurred during our simulation runs had little effect on brain P_{CO_2}. However, CSF P_{CO_2} only very slowly responded to changes in brain P_{CO_2}. Hence, if CSF P_{CO_2} were used in the controller function it would significantly slow centrally induced ventilation changes.

There have been numerous other models before those described above that have notable features. However, they will not be discussed here as Ursino *et al.*[47] and Topor *et al.*[46] have thoroughly reviewed them.

The model predictions have an inherent oscillation during simulated hypoxic conditions, a characteristic seen in virtually all previous models, including that of Grodins *et al.*[18] This behavior is first noticed in the predictions of Fig. 4, where during eucapnia, there are predicted overshoots and undershoots in both ventilation and alveolar P_{O_2} at the onset of breathing gases with low O_2 and just after breathing normal air again. The transient oscillations become much more extreme when P_{CO_2} is allowed to vary (Fig. 7). Hence, it is the peripheral interaction of CO_2 and O_2 in the controller formulation (Eq. 10) that plays the important role in producing this effect. At extreme conditions of high altitude, the system actually becomes unstable (see Fig. 10, lower panel). The dynamics of this predicted response to hypoxia depends upon the dynamics of the peripheral chemoceptor response which is most influenced by the 35-s time constant in that loop. This time constant was used to produce ventilatory transients consistent with neural afterdischarge.[15] The oscillation may have some relevance to breathing irregularities seen during sleep and at altitude, however the controller function used in the present study does not allow apnea to occur at low P_{CO_2} values. Hence, predictions of the present model probably don't pertain to classical periodic breathing.

Although we feel that the present model is the most completely validated of any published and quite adequate for description of respiratory responses to a number of important forcings, there are areas where it could be improved. The effect of gravity has not been included, hence, the effect of ventilation-perfusion inequalities in various lung zones cannot be investigated. The model does not include a simulation of respiratory mechanics and the respiratory cycle. In its current formulation, the model does not adequately describe alveolar-arterial O_2 dynamics during a rapid decompression where rapid movement of gases delays equilibration between blood and alveolar gas. The necessary improvements would entail simulating the diffusion dynamics of O_2. We would also like to look at longer-term effects of hypoxia where the HVD-phenomenon is important. An important issue not covered in the present model is the effect of metabolic acid–base disturbances[44] on longer-term respiratory control. Simulation of this phenomenon would require improvements in both the respiratory plant and the controller.

APPENDIX

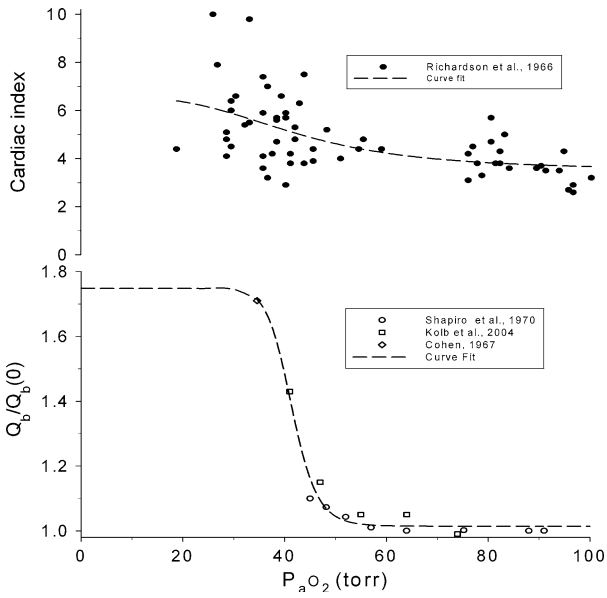

FIGURE A1. Cardiac index data (solid circles) from Richardson *et al.*,[39] upper panel, and the ratio of brain blood flow to its resting value (lower panel) from various sources (open symbols) are plotted against P_{aO_2}. The dashed lines are sigmoidal fits to the data. In Eq. (6), the fit was scaled so that cardiac output was unchanged at resting P_{AO_2}.

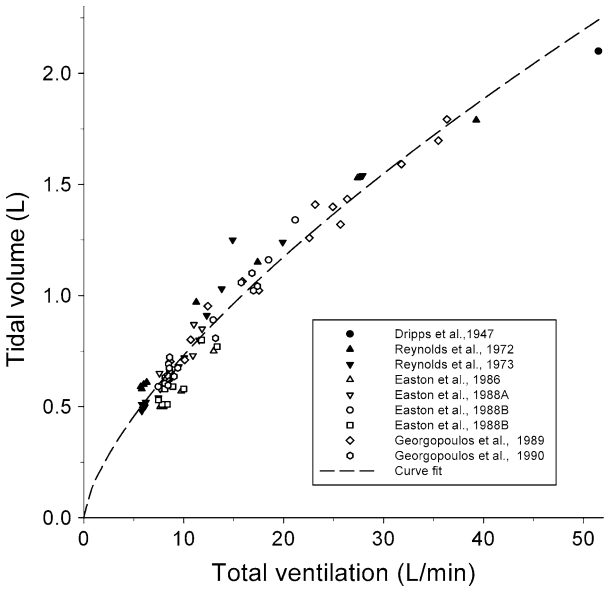

FIGURE A2. Tidal volume is shown as a function of total ventilation. Experimental data (symbols) are from various sources.[9,12–16,36,37] The curve fit (Eq. 13) is shown by the dashed line.

ACKNOWLEDGMENTS

We dedicate this paper to Dr. Fred Grodins first Chair of the Department of Biomedical Engineering at the University of Southern California. One of us (MBW) was a junior faculty member in this Department from 1967 to 1970. Although MBW was not involved at that time with respiratory physiology, he came away with a great appreciation for Fred's wisdom and his ability to simplify complex problems. We hope that Fred would approve of this work and see it as a significant contribution to understanding the control of respiration.

REFERENCES

[1]Bellville, J. W., B. J. Whipp, R. D. Kaufman, G. D. Swanson, K. A. Aqleh, and D. M. Wiberg. Central and peripheral chemoreflex loop gain in normal and carotid-body-resected subjects. *J. Appl. Physiol.* 46:843–853, 1979.

[2]Cohen, P. J., S. C. Alexander, T. C. Smith, M. Reivich, and H. Wollman. Effects of hypoxia and normocarbia on cerebral blood flow and metabolism in conscious man. *J. Appl. Physiol.* 23:183–189, 1967.

[3]Comroe, J. H. Jr Physiology of Respiration. Chicago: Year Book Medical Publishers, 1965.

[4]Cormack, R. S., D. J. C. Cunningham, and J. B. L. Gee. The effect of carbon dioxide on the respiratory response to want of oxygen in man. *Quar. J. Exp. Physiol. Cog. Med. Sci.* 42:303–319, 1957.

[5]Cullen, D. J., and I. E. I. Eger. Cardiovascular effects of carbon dioxide in man. *Anesthesiology* 41:345–349, 1974.

[6]Cunningham, D. J. C. The control system regulating breathing in man. *Quar. Rev. Biophys.* 6:433–483, 1974.

[7]Cunningham, D. J. C., P. A. Robbins, and C. B. Wolff. Integration of respiratory responses to changes in alveolar partial pressures of CO_2 and O_2 and in arterial pH. In: Section 3: The Respiratory System, edited by A.P. Fishman. Bethesda: American Physiological Society, 1986, pp. 475–528.

[8]Davenport, H. W. The ABC of Acid–base Chemistry. Chicago: The University of Chicago Press, 1958.

[9]Dripps, R. D., and J. H. Comroe Jr. The respiratory and circulatory response of normal man to inhalation of 7.6 and 10.4 per cent CO_2 with a comparison of the maximal ventilation produced by severe muscular exercise, inhalation of CO_2 and maximum voluntary ventilation. *Am. J. Physiol.* 149:43–51, 1947.

[10]Duffin, J. A mathematical model of the chemoreflex control of ventilation. *Resp. Physiol.* 15:277–301, 1972.

[11]Duffin, J., R. M. Mohan, P. Vasiliou, R. Stephenson, and S. Mahamed. A model of the chemoreflex control of breath in humans: model parameters measurement. *Resp. Physiol.* 120:13–26, 2000.

[12]Easton, P. A., and N. R. Anthonisen. Carbon dioxide effects on the ventilatory response to sustained hypoxia. *J. Appl. Physiol.* 64:1451–1456, 1988.

[13]Easton, P. A., L. J. Slykerman, and N. R. Anthonisen. Ventilatory response to sustained hypoxia in normal adults. *J. Appl. Physiol.* 61:906–911, 1986.

[14]Easton, P. A., L. J. Slykerman, and N. R. Anthonisen. Recovery of the ventilatory response to hypoxia in normal adults. *J. Appl. Physiol.* 64:521–528, 1988.

[15]Georgopoulos, D., Z. Bshouty, M. Younes, and N. R. Anthonisen. Hypoxic exposure and activation of the afterdischarge mechanism in conscious humans. *J. Appl. Physiol.* 69:1159–1164, 1990.

[16]Georgopoulos, D., S. Walker, and N. R. Anthonisen. Effect of sustained hypoxia on ventilatory response to CO_2 in normal adults. *J. Appl. Physiol.* 68:891–896, 1990.

[17]Gray, J. S. The multiple factor theory of the control of respiratory ventilation. *Science* 103:739–744, 1946.

[18]Grodins, F. S., J. Buell, and A. J. Bart. Mathematical analysis and digital simulation of the respiratory control system. *J. Appl. Physiol.* 22:260–276, 1967.

[19]Grodins, F. S., J. S. Gray, K. R. Schroeder, A. L. Norins, and R. W. Jones. Respiratory responses to CO_2 inhalation. A theoretical study of a nonlinear biological regulator. *J. Appl. Physiol.* 7:283–308, 1954.

[20]Grodins, F. S., and S. M. Yamashiro. Respiratory Function of the Lung and its Control. New York: Macmillan, 1978.

[21]Hall, F. G. Cabon dioxide and respiratory regulation at altitude. *J. Appl. Physiol.* 5:603–606, 1953.

[22]Hoffman, R. T., C. E. Clark Jr, and E. B. Brown Jr. Blood oxygen saturation and duration of consciousness in anoxia at high altitude. *Am. J. Physiol.* 145:685–692, 1946.

[23]Izraeli, S., D. Avgar, M. Glikson, U. Shochat, Y. Glovinsky, and J. Ribak. Determination of the 'time of useful consciousness' (TUC) in repeated exposures to simulated altitude of 25, 000 ft (7,620 m). *Aviat. Space Environ. Med.* 59:1103–1105, 1998.

[24]Kazemi, H., and J. C. Mithoefer. CO_2 dissociation curve of dog brain. *Am. J. Physiol.* 203:598–600, 1963.

[25]Khoo, M. C. K., R. E. Kronauer, K. P. Strohl, and A. S. Slutsky. Factors inducing periodic breathing in humans: a general model. *J. Appl. Physiol.* 53:644–659, 1982.

[26]Kolb, J. C., P. N. Ainslie, K. Ide, and M. J. Poulin. Protocol to measure acute cerebrovascular and ventilatory responses to isocapnic hypoxia in humans. *Resp. Physiol. Neurobiol.* 141:191–199, 2004.
[27]Liang, P., D. A. Bascom, and P. A. Robbins. Extended models of the ventilatory response to sustained isocapnic hypoxia. *J. Appl. Physiol.* 82:667–677, 1997.
[28]Lloyd, B. B., and D. J. C. Cunningham. A quantitative approach to the regulation of respiration. In: The Regulation of Human Respiration, edited by D. J. C. Cunningham and B. B. Lloyd. Oxford: Blackwell, 1963, pp. 331–349.
[29]Lobdell, D. D. An invertible simple equation for computation of blood O_2 dissociation relations. *J. Appl. Physiol.* 50:971–973, 1981.
[30]Longobardo, G., C. J. Evangelisti, and N. S. Cherniack. Effects of neural drives on breathing in the awake state in humans. *Resp. Physiol.* 129:317–333, 2002.
[31]Nielsen, M., and H. Smith. Studies on the regulation of respiration in acute hypoxia. *Acta Physiol. Scand.* 24:293–312, 1951.
[32]Patrick, W., K. Webster, A. Puddy, R. Sanii, and M. Younes. Respiratory response to CO_2 in the hypocapnic range in awake humans. *J. Appl. Physiol.* 79:2058–2068, 1995.
[33]Poulin, M. J., P.-J. Liang, and P. A. Robbins. Dynamics of the cerebral blood flow response to step changes in end-tidal PCO_2 and PO_2 in humans. *J. Appl. Physiol.* 81:1084–1095, 1996.
[34]Rahn, H., and A. Otis. Man's respiratory response during and after acclimatization to high altitudes. *Am. J. Physiol.* 157:445–462, 1949.
[35]Reivich, M. Arterial PCO_2 and cerebral hemodynamics. *Am. J. Physiol.* 206:25–35, 1964.
[36]Reynolds, W. J., and H. T. Milhorn Jr. Transient ventilatory response to hypoxia with and without controlled alveolar P_{CO2}. *J. Appl. Physiol.* 35:187–196, 1973.
[37]Reynolds, W. J., H. T. Milhorn Jr., and G. H. Holloman Jr.. Transient ventilatory response to graded hypercapnia in man. *J. Appl. Physiol.* 33:47–54, 1972.
[38]Richardson, D. W., H. A. Kontos, A. J. Raper, and J. L. Patterson Jr. Systemic circulatory responses to hypocapnia in man. *Am. J. Physiol.* 223:1308–1312, 1972.
[39]Richardson, D. W., H. A. Kontos, W. Shapiro, and J. L. Patterson Jr. Role of hypocapnia in the circulatory response to acute hypoxia in man. *J. Appl. Physiol.* 21:22–26, 1966.
[40]Richardson, D. W., A. J. Wasserman, and J. L. Patterson Jr. General and regional circulatory response to changes in blood pH and carbon dioxide tension. *J. Clin. Invest.* 40:31–43, 1961.
[41]Severinghaus, J. W. Proposed standard determination of ventilatory responses to hypoxia and hypercapnia in man. *Chest* 70(suppl 1):129–131, 1976.
[42]Severinghaus, J. W. Simple, accurate equations for human blood O_2 dissociation computations. *J. Appl. Physiol.* 46:599–602, 1979.
[43]Shapiro, W., A. J. Wasserman, J. P. Baker, and J. L. Patterson Jr. Cerebrovascular response to acute hypoxia and eucapnic hypoxia in normal man. *J. Clin. Invest.* 49:2362–2368, 1970.
[44]Somogyi, R. B., D. Preiss, A. Vesely, J. A. Fisher, and J. Duffin. Changes in respiratory control after 5 days at altitude. *Resp. Physiol. Neurobiol.* 145:41–52, 2005.
[45]Takahashi, E., and K. Doi. Destabilization of the respiratory control by hypoxic ventilatory depressions: a model analysis. *Jap. J. Physiol.* 43:612, 1993.
[46]Topor, Z. L., M. Pawlicki, and J. E. Remmers. A computational model of the human respiratory control system responses to hypoxia and hypercapnia. *Ann. Biomed. Eng.* 32:1530–1545, 2004.
[47]Ursino, M., E. Magosso, and G. Avanzolini. An integrated model of the human ventilatory control system: the response to hypercapnia. *Clin. Physiol.* 21:447–464, 2001.
[48]Ursino, M., E. Magosso, and G. Avanzolini. An integrated model of the human ventilatory control system: the response to hypoxia. *Clin. Physiol.* 21:465–477, 2001.